A PROTEOMIC STUDY OF OXIDATIVE STRESS IN ALCOHOLIC LIVER

DISEASE

A Thesis

by

BILLY WALKER NEWTON

Submitted to the Office of Graduate Studies of
Texas A&M University
in partial fulfillment of the requirements for the degree of

MASTER OF SCIENCE

May 2008

Major Subject: Chemical Engineering

A PROTEOMIC STUDY OF OXIDATIVE STRESS IN ALCOHOLIC LIVER DISEASE

A Thesis

by

BILLY WALKER NEWTON

Submitted to the Office of Graduate Studies of
Texas A&M University
in partial fulfillment of the requirements for the degree of

MASTER OF SCIENCE

Approved by:

Chair of Committee,	Arul Jayaraman
Committee Members,	Shashi Ramaiah
	Juergen Hahn
Head of Department,	Michael Pishko

May 2008

Major Subject: Chemical Engineering

ABSTRACT

A Proteomic Study of Oxidative Stress in Alcoholic Liver Disease. (May 2008)

Billy Walker Newton, B.S., Texas A&M University

Chair of Advisory Committee: Dr. Arul Jayaraman

Alcoholic steatosis (AS) is the initial pathology associated with early stage alcoholic liver disease and is characterized by the accumulation of fat in the liver. AS is considered clinically benign as it is reversible, as compared with alcoholic steatohepatitis (ASH) which is the next stage of alcoholic liver disease (ALD), and mostly irreversible. Proteomics were used to investigate the molecular basis of AS to determine biomarkers representative of AS. Liver tissue proteins at different stages of steatosis from a rodent model of AS were separated by two dimensional electrophoresis (2DE), followed by MALDI mass spectrometry (MS) identification of significantly expressed proteins. Expression levels of several proteins related to alcohol induced oxidative stress, such as peroxiredoxin 6 (PRDX6) and aldehyde dehydrogenase 2 (ALDH2) were reduced by 2 to 3-fold in ethanol fed rats, and suggested an increase in oxidative stress. Several proteins involved in fatty acid and amino acid metabolism were found at increased expression levels, suggesting higher energy demand upon chronic exposure to ethanol. In order to delineate between the effects of fat accumulation and oxidative stress, an *in vitro* hepatocyte cell culture model of steatosis was developed. HepG2 cells loaded with oleic acid surprisingly demonstrated lower cytotoxicity upon

oxidative challenge (based on lactate dehydrogenase activity) and inflammation (based on TNF-α induced activation of the pro-inflammatory transcription factor NF-κB). We also examined the effect of oleic acid loading in HepG2 cells on protein carbonylation, which is an important irreversible protein modification during oxidative stress that leads to protein dysfunction and disease. Fat-loaded hepatocytes exposed to oxidative stress with tert-butyl hydroperoxide (TBHP) contained 17% less carbonylated proteins than the non-fat loaded control. Mass spectrometric analysis of carbonylated proteins indicated that known classical markers of protein carbonylation (e.g., cytoskeletal proteins, chaperones) are not carbonylated in oleic acid loaded HepG2 cells, and suggests that the protective effect of fat loading is through interference with protein carbonylation. While counterintuitive to the general concept that AS increases oxidative stress, our fat loading results suggests that low levels of fat may activate antioxidant pathways and ameliorate the effect of subsequent oxidative or inflammatory challenge.

DEDICATION

I would like to dedicate this to my family and friends for all their love and support. Without them, this endeavor would not be possible.

ACKNOWLEDGEMENTS

I would like to extend my profound thanks to my committee chair, Dr. Arul Jayaraman, and my committee members, Dr. Shashi Ramaiah and Dr. Juergen Hahn, for their guidance and support throughout the course of this research.

I would to thank and acknowledge Dr. Shashi Ramaiah and Atrayee Banerjee for providing samples used in this experiment.

I would like to thank Towanna Hubacek, the department program coordinator for her help and support.

TABLE OF CONTENTS

LIST OF FIGURES

LIST OF TABLES

1. INTRODUCTION

The overall goal of this study is to elucidate the molecular basis of alcoholic steatosis (AS).   Chronic ingestion of alcohol leads to a sequence of hepatic pathologies associated with alcoholic liver disease (ALD), ranging from alcoholic steatosis (AS) to cirrhosis and liver failure (1-3). Steatosis or the accumulation of fat in the liver is the initial pathology that is common to all aspects of ALD. AS is generally considered clinically benign as it is reversible (i.e., fat accumulation can be reversed). On the other hand, the subsequent stages of ALD such as alcoholic steatohepatitis (ASH) and are mostly irreversible (2) . The progression of ALD to ASH represents a rate limiting step in the progression of ALD, because approximately 50% of individuals with ASH go onto develop end-stage liver diseases such as cirrhosis (2-4).

Although AS reverts upon alcohol withdrawal (5), research indicates that the accumulation of fat leads to subsequent liver complications, with the severity of damage being related to the extent of fat accumulation (6-8). Liver damage can have serious repercussions as steatotic livers are also highly vulnerable to infection, inflammation, or oxidative stress (9-11). Since, diagnosis and intervention at the AS stage has a higher likelihood of returning a patient to normal hepatic function, it is important to understand the mechanisms underlying AS in order to diagnose and develop therapies for treating ALD.

_____

This thesis follows the style of *Molecular and Cellular Proteomics.*

However, since the accumulation of fat itself can lead to some degree of oxidative stress, the interaction between these two factors is likely to be important in AS and early stage ALD. Therefore, investigating the effects of fat accumulation and oxidative stress, both individually and in combination, can lead to greater mechanistic understanding of AS and approaches for attenuating complications arising from AS.

One of the main difficulties associated with ameliorating fat accumulation in the liver is the lack of reliable diagnostic markers. Researchers have proposed carbohydrate dependent transferrin, which is known to be lower in alcoholics (12), and ethanol glucuronide (a direct ethanol metabolite) (13) as markers for early stage ALD. But neither of these accurately indicates the progression of AS or ASH. Proteomic studies have had great success in identifying prognostic and diagnostic markers for several diseases, including alcohol-related diseases, cerebral palsy, severe combined immunodeficiency, and Alzheimer's disease (14-17). Recently, two dimensional electrophoresis (2DE) based protein separation and quantification followed by MALDI-TOF MS-identification has been used to identify differentially expressed proteins from brains of alcohol preferring and alcohol non-preferring rats (18). This study and others indicate that a 2DE proteomics study has the potential in identifying early stage ALD markers. However, to-date no liver-enriched proteins have been identified from alcohol-treated liver.

We hypothesize that a comprehensive proteomic analysis of steatotic livers can lead to a fundamental understanding of AS as well as the identification of diagnostic markers for AS. Using an *in vivo* rodent model for AS and a two dimensional gel

electrophoresis (2DE) / matrix assisted laser desorption identification (MALDI) mass

spectrometry (MS) proteomics, we systematically investigated the protein basis

underlying AS. In parallel, we used an *in vitro* hepatocyte culture system to investigate

the effects of fat accumulation and oxidative stress independently. Since oxidative stress

also leads to irreversible modification of proteins (e.g., carbonylation) and cellular

dysfunction (19-22), we also used proteomic methods to establish the extent of protein

carbonylation and identify proteins that are carbonylated under conditions of oxidative

stress and steatosis.

2. BACKGROUND

2.1 Alcoholic Liver Disease

Alcohol abuse is a leading cause of health problems in the developed world. (23).
In the United States, alcoholism costs more than $185 billion and results in about
100,000 deaths per year (17). The liver is the most common target for alcohol and
chronic alcohol consumption leads to the development of alcoholic liver disease (ALD).
While, the pathogenesis of ALD has been extensively studied (2, 6, 24-27), far less is
known about the mechanisms underlying for the development and progression of ALD.
A complex relationship exists between the amount of alcohol consumption and the
likelihood of developing ALD (8), and there is considerable individual variability in the
development of alcohol related liver injury. The first major pathological condition in the
progression of ALD is alcoholic steatosis (fatty liver). Alcoholic steatosis (AS)
progresses gradually to alcoholic steatohepatitis (fatty liver combined with
inflammation), then to fibrosis, and ultimately cirrhosis (2). AS is thought to occur
rapidly upon alcohol consumption, but there is much less clarity on further progression
of ALD. Furthermore, evidence exists that alcohol alone may not be enough to cause
steatohepatitis and necrosis, and additional factors may be needed for the development
of disease (2, 27).

2.2 Alcoholic Steatosis and Alcoholic Steatohepatitis

Steatosis is the first and most common pathology in ALD and occurs in up to
90% of alcoholics. Fatty liver is thought to be mainly a result of metabolic disturbances,
such as decreased fatty acid oxidation, increased triglyceride synthesis, reduced fat

export, and mobilization of extrahepatic fat stores (28-31). The metabolism of ethanol to acetaldehyde, and its subsequent conversion to acetate produces NADH. The cellular accumulation of NADH increases substrate available for fatty acid synthesis, as well as disrupts mitochondrial beta oxidation, thereby leading to fat accumulation (32). Steatosis has long been considered a benign condition, as even severe cases of AS recovered after 3-4 weeks of alcohol withdrawal (5, 33, 34). However, more recent studies indicate that the metabolic changes taking place during the steatosis may also sensitize the cells to further injury (9, 12, 35, 36). Lieber (29) suggested that metabolic changes of fatty liver alone may be insufficient to cause inflammation. It is now believed that degree of fat accumulation in the liver correlates to the susceptibility of subsequent liver damage (6). Researchers have shown that fatty liver is highly vulnerable to oxidative stress or injury mediated by endotoxins or cytokines (9-11). While these studies show vulnerabilities of steatotic livers, one study also showed that a fatty liver induced by 5 weeks of ethanol exposure demonstrated enhanced capacity to regenerate and consequent decline in hepatic injury (37). This was not due to reduced CYP2E1 activity, but possibly through activation of the transcription factor NF-κB (37).

Evidence exists that alcohol alone may not be enough to cause steatohepatitis and necrosis, and further studies are needed to understand mechanisms of AS, and identify biomarkers leading to subsequent pathological stages of ALD (1). While, a detailed understanding of the mechanisms underlying the transition from AS to ASH is lacking, it is known continued consumption of alcohol in humans eventually results in neutrophilic steatohepatitis (38, 39). Neutrophil infiltration into the liver is hallmark of ASH and

contributes to the pathology of ALD. Alcoholic steatohepatitis reverts back to normal

hepatic histopathology approximately only 10% of the time (40). Most patients with

steatohepatitis (almost 50%) go on to develop fibrosis and cirrhosis (Figure 1).

Steatohepatitis, therefore represents a major rate limiting step in the progression towards

cirrhosis and clinical liver disease (2, 3). It would be beneficial to patients with ALD to

receive diagnosis and intervention before the onset of steatohepatitis

Progression of Alcoholic Liver Disease in Chronic Alcoholics

Normal Liver

27% 90-100%

Steatosis

10-35% 8-20%

Steatohepatitis → Fibrosis/Cirrhosis

40%
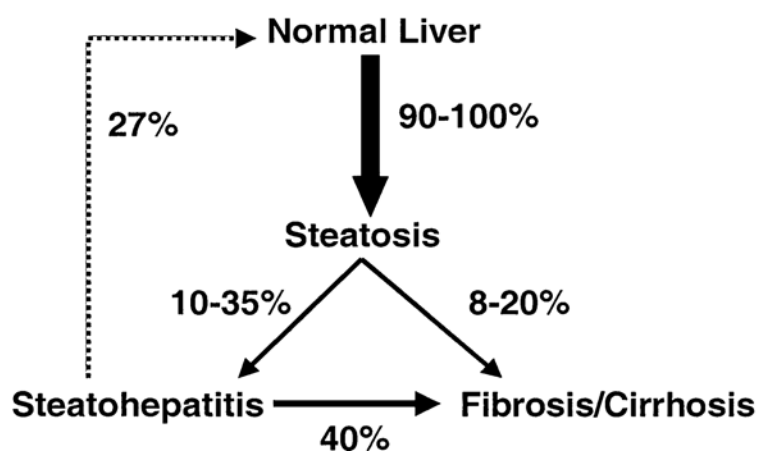
Figure 1. Progression of alcoholic liver disease. Consumption of ethanol
produces hepatic pathology in sequence, ranging from steatosis (fatty liver) on
one extreme, to fibrosis/cirrhosis on the opposite end of the spectrum (1).

2.3 Alcohol Metabolism and Oxidative Stress

The generation of reactive oxygen species (ROS) is an unavoidable consequence

of aerobic respiration. Superoxide ($O_2^{\cdot-}$) is a major ROS generated from electron

transport processes (e.g. ATP synthase I, and cytochrome p450), as well as various

oxidase enzymes. Evidence for the role of $O_2^{.-}$ in ALD comes from the studies demonstrating an inverse relationship between superoxide dismutase (SOD) and liver injury (41). SOD is an enzyme that reduces $O_2^{.-}$ to hydrogen peroxide (H_2O_2). Kessava et al. (42) showed that SOD1 knockout mice develop more severe liver damage after treatment with ethanol. While $O_2^{.-}$ is not a potent oxidant, it reacts catalytically with enzyme metal centers to produce more potent oxidants such as hydroxyl radical ($OH^.$) (43), hypochlorous acid (HOCl) (44), and peroxynitrite ($ONOO^-$) (45). Under basal conditions cells have adequate antioxidant systems to deal with the ROS generated during normal cellular processes, however consumption of alcohol is thought to cause metabolic changes that leads to increased oxidative stress, such that the generation of ROS begins to overwhelm cellular antioxidant systems.

Three main mechanisms explain the effects of alcohol on oxidative stress (1). The direct metabolite of alcohol is acetaldehyde, which is a very reactive compound. The accumulation of acetaldehyde is thought to be primarily responsible for symptoms of alcohol ingestion, as it has been shown to form adducts with biomolecules such as lipids (16). Metabolism of ethanol and acetaldehyde also reduces NAD^+ to NADH, and the shifting of this $NADH/NAD^+$ ratio greatly reduces NAD^+ available for carbohydrate and lipid metabolism. This decrease in metabolic rate reduces the available cellular ATP pool (46) and limits energy available to antioxidant pathways; thereby, indirectly leading to greater accumulation of ROS. In addition, ethanol also activates the CYP2E1 pathway for the metabolism of ethanol, which leads to increased ROS generation (47).

2.4 Effects of Oxidative Stress

Oxidative attack on proteins by ROS can lead to reversible or irreversible changes. The ROS associated with oxidative stress causes cellular damage by attacking several cellular components such as lipids and proteins. Hydroxyl radicals can damage lipids through a process called lipid peroxidation (48). Malondialdehyde is an end product of lipid peroxidation that has been used as a biomarker for oxidative stress (48). Proteins are also commonly subject to modification by ROS. While some of these changes are considered harmless, others may lead to inactivation of the protein. Irreversible proteins modifications tend to inactivate proteins and lead to permanent cellular damage (49). Reversible modifications such as s-glutathionylation, s-nitrosation, and methionine sulfoxidation may not be entirely unintentional and may serve dual purposes. These modifications may serve to protect proteins by blocking sensitive residues from irreversible oxidation and also modulate protein function (redox regulation and signaling) (49-51).

Protein carbonylation is the largest class of irreversible protein modification. Carbonylation is characterized as the non-enzymatic irreversible modification of proteins by a variety of oxidative pathways that results in the addition of carbonyl group. Protein carbonylation occurs mainly by direct oxidation of the side chains of lysine, arginine, proline, and threonine.
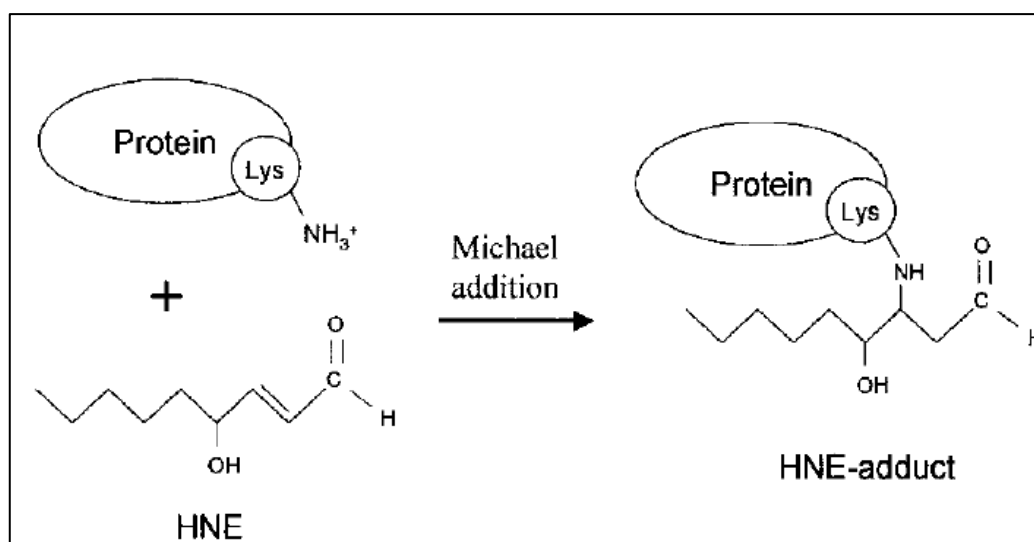
Figure 2. Covalent addition of lipid peroxidation product, 4-HNE. This is a major source of protein carbonylation.

Covalent addition of lipid peroxidation products such as 4-hydroxy-2-nonenal (HNE) (13) to lysine, histidine, and cystine or n-terminal residues is also a major source of carbonylation, as shown in Figure 2. Protein carbonylation is especially damaging since cells are unable to repair them and leads to either removal of the modified protein via the ubiquitin/proteasomal system or aggregation. There are many examples relating carbonylation to protein dysfunction. In the mitochondria of *Drosophila melanogaster*, the activity of enzymes such as acotinase and adenine nucleotide translocase was found to be inhibited with an increase in carbonylation (52-54). Carbonylation was also found to interfere with chaperone function and protein folding (55, 56). There is much evidence that oxidative stress is involved in many disease states, such as aging (57), and the irreversible nature of protein carbonylation makes it an attractive target of study.

3. MATERIALS AND METHODS

3.1 Reagents and Supplies

Two dimensional electrophoresis (2DE) gel strips were purchased from (Bio-Rad Laboratories, Hercules, CA). All reagents and supplies for two dimensional gel electrophoresis (2DE) buffers, cell lysis buffers, and SDS-PAGE were purchased from Fisher Scientific (Hampton, NH), unless otherwise noted. Deoxyribonuclease (DNase), ribonuclease (RNase), iodoacetamide, and oleic acid were purchased from MP Biomedical (Solon, Ohio). Cell culture media and reagents were purchased from Hyclone, (Logan, UT), unless otherwise noted.

3.2 Animals

Rat livers used in this study were provided by the laboratory of Dr. S. Ramaiah (Dept. of Veterinary Pathobiology, Texas A&M University, College Station TX). Procedures followed for rats were as follows. Male Sprague-Dawley rats (220-250 g) were purchased from Harlan Sprague Dawley, (Houston, TX). Male Sprague-Dawley rats were housed individually in cages in a temperature-controlled animal facility with a 12-h light-dark cycle. Rats were utilized after a 1-week equilibration period. Rats were divided into two groups (n=20 each), control diet group and experimental diet group. Rats in the experimental group were further divided into a group fed for 3 weeks and a group fed for 6 weeks. The experimental groups were then placed on a Lieber DeCarli AS diet model (37, 58, 59). The rats were fed either control (isocaloric control diet where the calories were adjusted with maltose-dextrin) or EtOH-containing (35.5% of total calories) Lieber-DeCarli diet (Bio-Serv, Frenchtown, NJ) for a period of six weeks

for the control and three or six weeks for the EtOH groups, respectively. For the first day, rats received plain liquid diet; next, alcohol-treated rats received liquid diet containing alcohol to 2% and 4% (w/v), each for 2 days. The 4% alcohol diet was then continued for six weeks. The energy distribution from the EtOH liquid is as follows; 18% protein, 35% fat and either 47% carbohydrate (control group) or 11.5% carbohydrate (maltose dextrin) and 35.5% EtOH (EtOH fed groups). The food consumption was recorded daily and the control rats were pair-fed according to the food consumption of EtOH-fed rats. Rats were weighed at the beginning of the study and weekly thereafter. Calories consumed by each rat were measured daily. Rats were sacrificed at the end of 3 and 6 weeks respectively (n=10) by CO2 asphyxiation. An additional control group (n=10 each, 4% chow) was also employed. No significant difference in body weight gain was observed between isocaloric controls and EtOH fed rats. Livers were harvested from the animals and perfused with phosphate buffered saline (PBS) before being frozen at -80 ˚C until needed.

3.3 Cell Culture

HepG2 cells (ATTC, Manassas, VA) were cultured in media containing 9.6 g/l modified eagle medium/Earle's balanced salt solution (MEM/EBSS) powdered media, 1.62 g/l sodium bicarbonate, 110 mg/l sodium-pyruvate, 10% fetal bovine serum, 200 units/ml penicillin, and 200 μg /ml streptomycin. Cells were maintained at 37 ˚C under a humidified 5% CO_2 environment. H35 rat hepatoma cells with a NF-κB reporter plasmid (H35 NF-κB) (60) were cultured in Dulbecco's minimal eagle's medium supplemented with 10% bovine serum, 200 units/ml penicillin, and 200 μg /ml

streptomycin. This cell line was generated by stably inserting a DNA fragment consisting of four tandem repeats of the NF-κB DNA binding sequence upstream of the CMV-minimal promoter and a 2h half-life variant of the enhanced green fluorescence protein (d2EGFP) (60).

3.4 Two Dimensional Electrophoresis

Liver tissue samples were homogenized in a standard two dimensional electrophoresis (2DE) buffer consisting of 2M thiourea, 7M urea, 4 wt% CHAPS, 50 mM DTT, 0.5 vol% ampholytes (pH 3-11) (Bio-Rad Laboratories, Hercules, CA). One tablet of Complete Mini™ protease inhibitor cocktail (Roche, Basel, Switzerland) was added to 10 ml buffer. Nuclease stock solution was prepared that contained 100 mM Tris pH 7, 50 mM MgCl, RNase 0.5 mg/ml, and DNase 1.0 mg/ml. After homogenizing, nuclease stock was added 1:10 to the 2DE buffer. The homogenate was centrifuge at 13000 rcf for 15 min, after which the supernatant was collected and the protein concentration determined by the BCA assay (Bio-Rad). The sample was further processed using the 2DE ReadyPrep (Bio-Rad) clean up kit per the manufacturer's instructions.

Homogenized supernatants were diluted in a buffer containing 9.5 M urea, 2 wt% CHAPS, 18 mM DTT, and 0.5 % ampholytes. Two sizes of immobilized pH gradient (IPG) strips (pH 5-8) (Bio-Rad) were used during the experiment. All spot detection and image analysis were done using 7cm strips, while 13.5 cm strips were used for gels for excising spots for MS analysis. 40 μg of protein was loaded onto 7 cm strips and 300 μg was loading onto 13.5 cm strips. After a minimum of 16 hrs of rehydration, isoelectric

focusing (IEF) was carried out on a Protean IEF cell (Bio-Rad) in 3 steps: 250V for 15 minutes, followed by a linear gradient of 250V – 4000V for one hour, and then 4000V for 5 hours. Proteins in the IPG strips were then reduced with DTT and alkylated with iodoacetamide in SDS equilibration buffer for fifteen minutes each as previously described (55). SDS-PAGE was conducted on 10% acrylamide gels at 125V for 70 minutes. Seven cm gels were fixed for 15 minutes in solution containing 20% methanol and 7% acetic acid and stained with Sypro Ruby stain (Invitrogen, Carlsbad, CA) overnight. The 13.5 cm gels were stained with GelCode Coomassie stain (Pierce, Rockford, IL). Gels were imaged using a VersaDoc 3000 imager (Bio-Rad), and image analysis was conducted using PDQuest 7.4 software (Bio-Rad). After imaging and analysis, statistically significant differentially expressed protein spots were selected for excision.   Spots were manually excised from the 13.5 cm gel with a 1 ml pipette, subjected to in-gel digestion using sequencing grade trypsin (Promega, Madison, WI), as previously described (61), and then used for MALDI-TOF-MS analysis.

3.5 MALDI Mass Spectrometry

Trypsin-digested protein spots were spotted onto MALDI targets using a ProMS™ robot capable of sample cleanup prior to MALDI-MS analysis (Genomic Solutions, Ann Arbor, MI). The MALDI-MS experiments were performed in a 4700 Proteomics Analyzer MALDI-TOF/TOF (Applied Biosystem, Foster City, CA). Twenty tandem MS spectra per spot were acquired. All MS and MS/MS data were queried against the Swiss-Prot protein sequence database using the GPS Explorer (Applied Biosystems) software. The parameters for database searching were as follows:

taxonomy, *Rattus Norvegicus*; database, Swiss Prot; enzyme, trypsin; maximum missed cleavages, 1; variable modifications, oxidation (Met); peptide tolerance, 85 ppm; and MS/MS fragment tolerance, 0.3 Da. The generated MALDI-MS data was confirmed by re-analyzing five spots.

3.6 *In vitro* Fat Loading Model

Fat loading of HepG2 cells was done by exposing cells at ~ 70% confluency to 1.0 mM oleic acid for 48 hr. An oleic acid stock solution (75 mM) was prepared by mixing oleic acid with a solution of 3 mg/ml solution of bovine serum albumin and 75 mM sodium hydroxide, with vortexing and heating to aid in dissolution of oleic acid. The solution was sterilized by passing through a 0.22 micron syringe filter. The stock solution dissolved into culture media at desired final media concentrations.

The extent of fat loading was assessed by oil red O staining. An oil red O (Alfa Aesar, Ward Hill, MA) stock solution was made by dissolving 0.7 g oil red O in 200 ml isopropanol and passing mixture through a 0.22 μm syringe filter. Oil red O working solution was prepared by combining four parts deionized water with six parts oil red O stock solution and passing through a syringe filter. Cultured cells were fixed with 10% formalin in phosphate buffered saline for 2 h, with the buffer being replaced with fresh formalin containing buffer after the first 10 minutes. After the formalin solution was removed, cells were rinsed with 60% isopropanol and allowed to dry. The oil red O working solution was added to cells and incubated for 10 minutes. The cells were rinsed with water to remove excess stain, dried briefly, and then imaged.

3.7 Oxidative Challenge Experiments with Tert-Butyl Hydroperoxide

Oxidative challenge experiments were conducted on fat-loaded and non fat-loaded HepG2 cells at approximately 85%-90% confluency.   Standard media was repaced with low serum media containing 1% fetal bovine serum. Tert-butyl hydroperoxide (TBHP) (Acros Organics, Geel, Belgium) was added to the media at the desired final concentrations. After an 8 hr exposure, culture supernatants were removed, and stored at -20 °C. The culture flasks were rinsed with PBS and frozen at -80 ˚C until further processing.

3.8 LDH Cytoxicity Assay

Lactate dehydrogenase (LDH) levels in supernatants from fat-loaded and TBHP exposed HepG2 cells were measured using the Cytotox-One LDH cytoxicity assay (Promega, Madison, WI). Equal volumes (100 μl) of culture supernatant and cytoxicity assay buffer were combined and incubated according to the manufacturer's instructions. LDH measurements were made in replicate for each cell exposure condition.

3.9 NF-κB Reporter Assays and Fluorescence Microscopy

H35 NF-κB cells were grown in 6 well plates (Corning, NY) and loaded with 0.15 or 0.90 mM oleic acid as described above for HepG2 cells. Reporter cells were exposed to 25 ng/ml TNF-α (R&D Systems, Minneapolis, MN) for 24 hrs in triplicate. GFP measurements were made using an Axiovert 200M fluorescence microscope (Zeiss, Thornwood, NY). Cell culture dishes were placed in a controlled environment chamber in the microscope and maintained at 37 ˚C and 10% CO2 throughout the experiment. Multiple imaging locations (3 per culture well) were randomly selected and the positions

marked before the addition of TNF-α using the 'mark and find' feature of the using the Zeiss AxioVision imaging software. Fluorescence and phase contrast images were obtained at the marked positions throughout the duration of the experiment using a 20X objective every 1 h for 24 h using an AxioCam MrM digital camera.

3.10 Biotin Tagging of Carbonylated Proteins

Carbonylated proteins from whole cell extracts were linked to biotin hydrazide following the protocol described by Mirzaei et al. (20, 21). HepG2 cells (~5x10^6 cells) were lysed with 600 μl of lysis buffer (0.1 % w/v SDS, 0.5 % w/v sodium deoxycholate, 1.0 % w/v CHAPS, 0.1 M NaCl, 0.1 M sodium phosphate, 1 mM EDTA; pH 7.5), supplemented with 80 μl nuclease stock solution (100 mM sodium bicarbonate pH 7, 50 mM MgCl, RNase 0.5 mg/ml, and DNase 1.0 mg/ml), 10 μl of mammalian protease inhibitor cocktail (Sigma Aldich, St. Louis, MO), and 70 μl of 50 mM biotin hydrazide (Pierce, Rockwell, IN) stock solution in DMSO. Half of this lysis solution was added to the cells, and incubated for 15 minutes, and the lysate collected. This step was repeated with the remaining lysis solution. The lysate was incubated for 30 minutes with 15 μM sodium cyanoborohydride (Fisher Scientific, Hampton, NH) to reduce hydrazone bonds. The lysate was incubated for at least 30 minutes, passed through a 22 gauge needle ten times, and centrifuged at 13000 rcf for 8 mins at 4 ˚C. The supernatant was collected and dialyzed to remove detergents and excess reagents.   Dialysis cassettes (2.0K MWCO, 0.5-2.0 ml) were purchased from Pierce and hydrated for 2 minutes in dialysis buffer containing 25 mM ammonium bicarbonate (pH 8.0) and 4 mg/ml BSA. Cell lysates were added to the cassettes per manufacturer's instructions, and the lysates were

dialyzed for two hours after which the buffer was replaced with fresh dialysis buffer.

The buffer was replaced again after two hours, and then dialyzed for at least eight hours.

The concentration of carbonylated protein in the dialyzed lysate was assayed by the

Bradford assay (Bio-Rad).

3.11 Affinity Purification of Carbonylated Proteins

One ml of monomeric avidin beads (Pierce, Rockford, IL) was placed in a 5 ml

centrifuge column (Pierce). In order to bind non-reversible sites, the column was

washed by adding 3 ml of elution buffer containing 2 μM biotin and 25 mM ammonium

bicarbonate, vortexing the beads, centrifuging at 1000 rcf for 45 seconds. The washing

step was repeated twice, and the column regenerated by washing three times with 3 ml

of regeneration buffer containing 0.1 M glycine, pH 2.8.   The column was then washed

four times with 3 ml of 25 mM ammonium bicarbonate. The dialyzed sample was added

to the column and incubated at room temperature for one hour with gentle vortexing

every 20 minutes and then centrifuged. The column was then washed 4 times with 3 ml

of 25 mM ammonium bicarbonate to remove nonspecifically bound proteins. The

biotinylated carbonylated proteins were eluted of the column by washing the beads five

times with 0.7 ml of the elution buffer. The flow-through was collected and then

lyophilized, using a Centrivap concentrator and cold trap (Labconco, Kansas City, MO).

3.12 Carbonylated Protein Detection and LC/MS/MS Sample Preparation

Lyophillized carbonylated proteins were rehydrated either in 50 μl of 25 mM ammonium bicarbonate for quantification using the Bradford assay or in 40 μl of reducing SDS-PAGE buffer (62) and resolved on a 7 cm 10% acrylamide gel. Gels were fixed for 15 minutes in solution containing 20% methanol and 7% acetic acid and stained with Sypro Ruby stain overnight. Stained gels were imaged using a VersaDoc imager (Bio-Rad) and gel lanes were manually excised and cut into 36 gel slices. The gel slices were used for robotic in gel digestion and mass spectrometry analysis.

3.13 LC MS/MS Analysis

Peptides from each gel slice were separated using reverse phase chromatography on a 150 μm X 10cm column (Vydac) using an LC-Packings autosampler and pumps (LC Packings, Sunnyvale, CA). A gradient of 2-40% acetonitrile was used to elute the peptides from the column at a flow rate of 1 μL/min. MALDI matrix (5mg/mL α-cyano-4-hydroxycinnamic acid) was mixed with the column eluant through a "T" junction at 1.4 μl/min and spotted directly onto a MALDI sample plate using an LC-Packings Probot. All MALDI-MS experiments were performed using a 4800 Proteomics Analyzer (Applied Biosystems). Data were acquired with the reflectron detector in positive mode (700-4500 Da, 1900 Da focus mass) using 800 laser shots (40 shots per sub-spectrum) with internal calibration. Collision induced dissociation tandem MS spectra were acquired using air at the medium pressure setting as the collision gas with 1 kV of collision energy. All MS and MS/MS data were searched against the Swiss-Prot protein sequence database using the GPS Explorer (Applied Biosystems) software.

4. RESULTS

4.1 Two Dimensional Gel Electrophoresis

Two Dimensional Electrophoresis (2DE) was used to investigate changes in the rat liver proteome during alcoholic steatosis generated using the Lieber-DiCarli model. Liver proteins were extracted from animals in a six weeks ethanol fed group, a three weeks ethanol fed group, and a control group, and separated by 2DE as described in Materials & Methods. In order to account for biological variability, liver tissue from three animals was included in each experimental group, and each tissue sample was processed in duplicate (for a total of 6 gels per experimental group). Based on preliminary optimization results (not shown), first dimension isoelectric focusing (IEF) strips were loaded with 40 μg of protein. Second dimension gels were stained with a fluorescent stain (Sypro Ruby) because of its sensitivity and broad dynamic range. Under these separation conditions, a total of 175 spots were detected on all gels. Representative gel images from each experimental group are shown in Figures 3A – C. A composite master gel was generated using the PDQuest image analysis software (Bio-Rad) in which protein spot features present in all the gels were imported onto a single synthetic gel (Figure 3D).

The intensity of each protein spot (i.e., spot volume) was normalized to the spot volume of the entire gel (i.e., of all the protein spots). Statistically significant changes in protein expression were determined using two sequential data analysis criteria. First, a protein spot had to be present in a minimum of 4 out of 6 gels for each sample to be included in the analysis. Next, protein spots were analyzed based on the fold-change in

expression. A protein spot in a gel from the ethanol-treated group was determined to

exhibit a statistically significant change in expression if its spot volume was 1.3-fold

different (increased or decreased) relative to the control group. The 1.3 fold change

(plus/minus) value was the lowest fold-change that was different from the untreated

control by one standard deviation (i.e. 67% confidence limits). This analysis resulted in

21 spots (corresponding to 18 proteins) being classified as differentially expressed in

ethanol-treated groups relative to the control group.
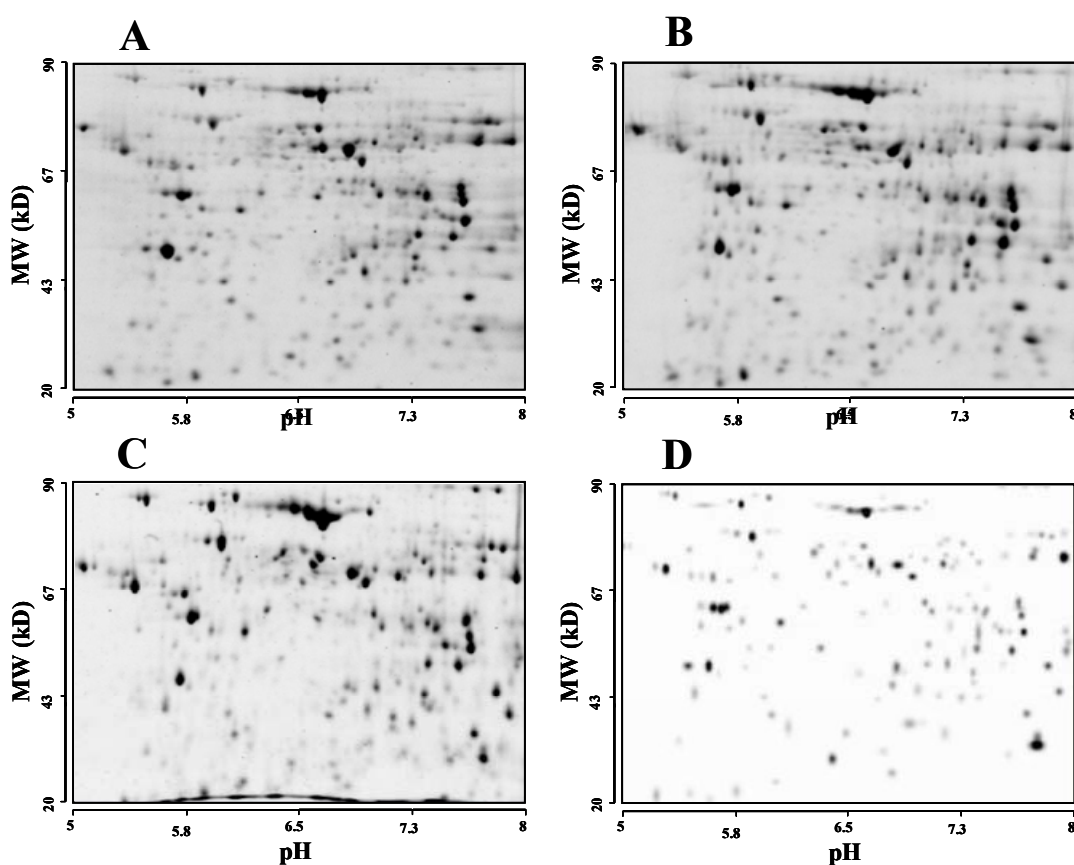
Figure 3. Representative 2DE gel images from steatotic livers. A. isocaloric control group, B. 3 weeks ethanol fed group, C. 6 weeks ethanol fed group, D. composite master gel image.

Proteins determined as differentially expressed were identified using MALDI-TOF mass spectrometry. In order to facilitate excision of protein spots, a 13 cm IEF strip was loaded with 350 μg of protein. Second dimension was performed using 11 cm Criterion precast gels (BioRad) and stained with Gelcode Blue stain for visualization. Protein spots were manually excised by comparing to the 7 cm gel images, digested with trypsin, purified, and analyzed using mass spectrometry. All of the excised proteins spots resulted in a positive identification, with most protein scores over one hundred.

Figure 4. Composite master gel image with annotated up or down regulated proteins.

The identified differentially expressed proteins are shown in Table 1. Figure 4 is a composite master gel image with annotated up or down regulated proteins. The proteins can be identified from their SSP numbers, which are listed in Table 1.

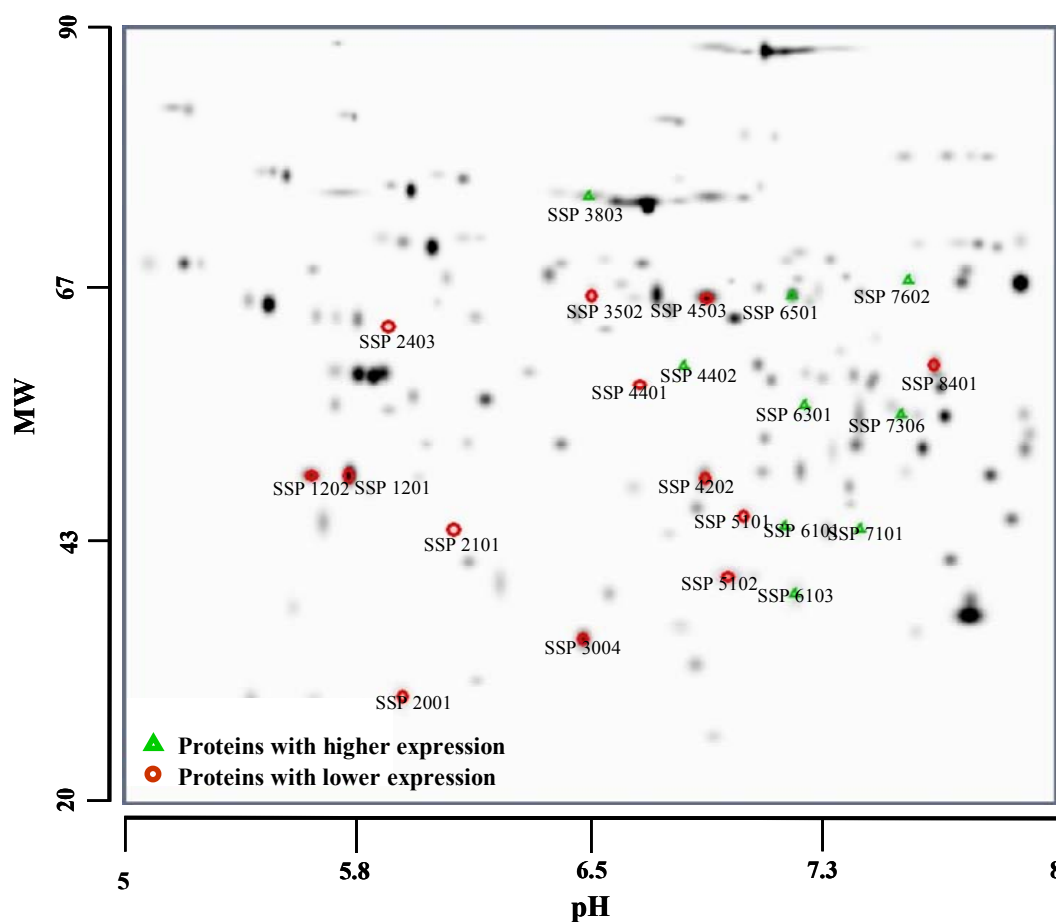Two trends are evident in the proteome data. First, a majority of differentially expressed proteins were mitochondrial proteins involved in amino acid and fat metabolism, chaperone proteins. This is not surprising, as the mitochondria are well established as an important site for oxidative damage; therefore, any treatment that generates 'stress' is expected to be reflected in the mitochondrial proteome. Second, proteins differentially expressed at 6 weeks were also significantly altered at 3 weeks as well, indicating that alterations in protein expression seen with steatosis are initiated at an early stage during ethanol exposure.

The up-regulation of proteins involved in fat and amino acid metabolism was observed. Acyl-CoA dehydrogenase and delta3,5-delta2, 4-dienoyl-CoA isomerase are both involved in mitochondrial beta oxidation of fatty acids (63, 64), with the former enzyme catalyzing the first step in the process. Similarly, 3-hydroxyisobutyrate dehydrogenase is an oxidoreductase that acts on CH-OH group of donors and is involved in leucine, isoleucine, and valine catabolism (65), while 2-oxoisovalerate dehydrogenase is an oxidoreductase that acts on aldehyde or oxo-group of donors (65). ADP/ATP translocase 2 is increased in expression, which catalyzes the exchange of ADP and ATP across the mitochondrial membrane.

Table 1. Differentially expressed proteins in normal and steatotic livers.

Protein Name	Accession No.	Protein Score	SSP No.	Fold Change Over Control Group	
				3 Weeks Ethanol Group	6 Weeks Ethanol Group
Senescence marker protein-30 (SMP-30) (Regucalcin)	Q03336	588	1201	-1.85	-1.71
Myosin Va (Myosin 5A) (Dilute myosin heavy chain, non-muscle)	Q9QYF3	50	1202	-2.51	-2.25
Phosphatidylethanolamine-binding protein (PEBP)	P31044	531	2001	-1.53	-2.01
Hsc70-interacting protein (Hip) (Putative tumor suppressor ST13)	P50503	87	2403	-1.21*	-1.92
Isocitrate dehydrogenase [NADP] (cp)	P41562	786	8401	-2.04	-1.89
Ketohexokinase (EC 2.7.1.3) (Hepatic fructokinase)	Q02974	364	5101	-1.53	-1.56
Endoplasmic reticulum protein ERp29 precursor (ERp31)	P52555	643	5102	-1.57	-1.80
Plectin 1 (PLTN) (PCN)	P30427	62	4202	-1.99	-1.65
Adenosine kinase (AK)	Q64640	238	4401	-1.77	-1.28*
Peroxiredoxin 6 ((Antioxidant protein 2)	O35244	856	3004	-1.33	-1.62
3-hydroxyanthranilate 3,4-dioxygenase(3-HAO)	P46953	729	2101	-1.61	-1.50
Aldehyde dehydrogenase (ALDH 2)	P11884	218	3502	-2.36	-1.97
Aldehyde dehydrogenase (ALDH 2)	P11884	713	4503	-1.49	-1.70
Serum albumin precursor	P02770	581	3803	1.70	1.90
Plectin 1 (PLTN) (PCN)	P30427	51	6103	10.99	11.93
3-hydroxyisobutyrate dehydrogenase, (HIBADH) (mp)	P29266	356	6101	1.64	1.33
ADP/ATP translocase 2	Q09073	58	6501	3.49	3.43
Acyl-CoA dehydrogenase, short-chain specific, (SCAD) (mp)	P15651	551	7306	1.47	2.30
Acyl-CoA dehydrogenase, short-chain specific, (SCAD) (mp)	P15651	102	6301	9.29	13.58
Delta3,5-delta2,4-dienoyl-CoA isomerase, (mp)	Q62651	147	7101	1.69	2.07
2-oxoisovalerate dehydrogenase (mp)	P11960	645	4402	3.48	2.77
Glutamate dehydrogenase, (GDH) (mp)	P10860	488	7602	1.73	1.67

Note: marked entries were lower then 1.3 fold change cut-off.

Interestingly, both aldehyde dehydrogenase (ALDH2) and peroxiredoxin 6 (PRDX6) were found to be down-regulated in the ethanol group as compared to the control. In the liver, ethanol is first converted to acetaldehyde, which is thought to be more toxic than ethanol itself (47). ALDH2 is the enzyme responsible for metabolizing acetaldehyde to acetic acid; therefore, its down-regulation suggests an accumulation of acetaldehyde and increasing hepatotoxicity. PRDX6 is an important antioxidant enzyme that is involved in cellular redox regulation (66). Specifically, PRDX6 reduces H_2O_2 and phospholipid hydroperoxides and is an important mediator in the protection against oxidative injury. The decrease in PRDX6 expression is indicative of increased oxidative stress in the liver after 3 and 6 weeks of ethanol consumption.

While one would expect an increase in the expression of anti-oxidant systems during oxidative stress, prior reports have shown that a decrease in anti-oxidant enzymes itself is an indicator of oxidative stress. This is because reactive oxygen species (ROS) are constantly generated in the cell during metabolism and are scavenged by anti-oxidant systems. This equilibrium is disturbed when there is an increase in the production of ROS, which leads to oxidative stress. This, in turn, leads to down-regulation of anti-oxidant systems, and further increases ROS levels and oxidative stress. Therefore, the down-regulation of PRDX6 is indicative of hepatocellular damage and increased ROS levels in the ethanol-treated group.

4.2 *In vitro* HepG2 Fat Loading Model

Our data, combined with previous work implicating fat accumulation and oxidative stress with ALD (6-8), motivated the development of an *in vitro* experimental model that would allow independent investigation of the effects fat loading and oxidative stress in hepatocytes. A fat loading hepatocyte cell culture model was developed with oleic acid as the model fatty acid because it has been reported to have the least toxicity to cells (67, 68).

A fat loading solution (sodium oleate) was developed as described in Materials & Methods to produce a solution that dissolved easily in media and did not significantly alter media pH. Oil red O staining was used to verify that hepatocytes were loaded with fat, as shown in Figure 5. The data show significant lipid accumulation after 48 h exposure with no obvious loss of viability, and indicates this model can be used for generating steatotic hepatocytes.
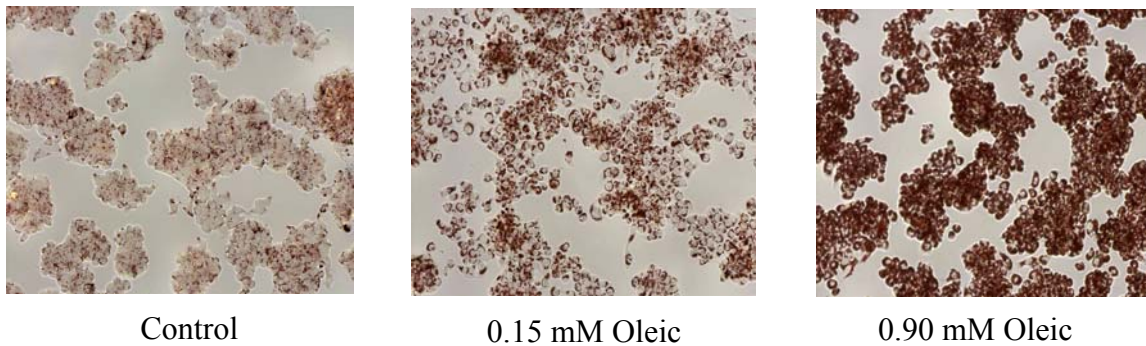

| Control | 0.15 mM Oleic | 0.90 mM Oleic |

Figure 5. Fat accumulation in oil red O stained HepG2 cells. Cells were exposed to indicated oleic acid concentration for 48 hours.

In order to simulate the effect oxidative stress during AS, fat loaded hepatocytes were initially exposed to a direct oxidant such as hydrogen peroxide. However, it is likely that H_2O_2 is rapidly scavenged by hepatocytes which possess extensive catalase and peroxidase enzymes (69), and much higher concentrations may be required to generate oxidative stress. Therefore, we used TBHP as the pro-oxidant molecule instead of H_2O_2. Since TBHP is not a substrate of catalase, it allows for greater generation of hydroxyl radicals (69). Since, oxidant exposure times beyond 6-8 hrs begin to show signs of apoptosis in many cells (69). Therefore, an exposure time of 8 hr with 500 μm TBHP was chosen for subsequent experiments.

4.3 Cytotoxicity in Fat-loaded HepG2 Cells

The LDH assay is a standard method of measuring the cytotoxicity of many chemicals. Fat- loaded and non fat-loaded HepG2 cells were either exposed to TBHP or to blank buffer. Reduced serum media (1% vs. 10%) was used to conduct the exposure experiment, as prior reports (69) have suggested that serum components may quench the applied oxidative stress. Figure 6 shows that fat-loaded cells have lower levels of LDH in the culture supernatant, both in the presence and absence of TBHP. Since LDH is a marker for cell membrane integrity, these results suggest that oleic acid-loaded HepG2 cells are less susceptible to pro-oxidant damage as compared to normal cells. These results are somewhat surprising, as several studies have suggested that fat accumulation is cytotoxic, especially under conditions of oxidative stress (6-8).
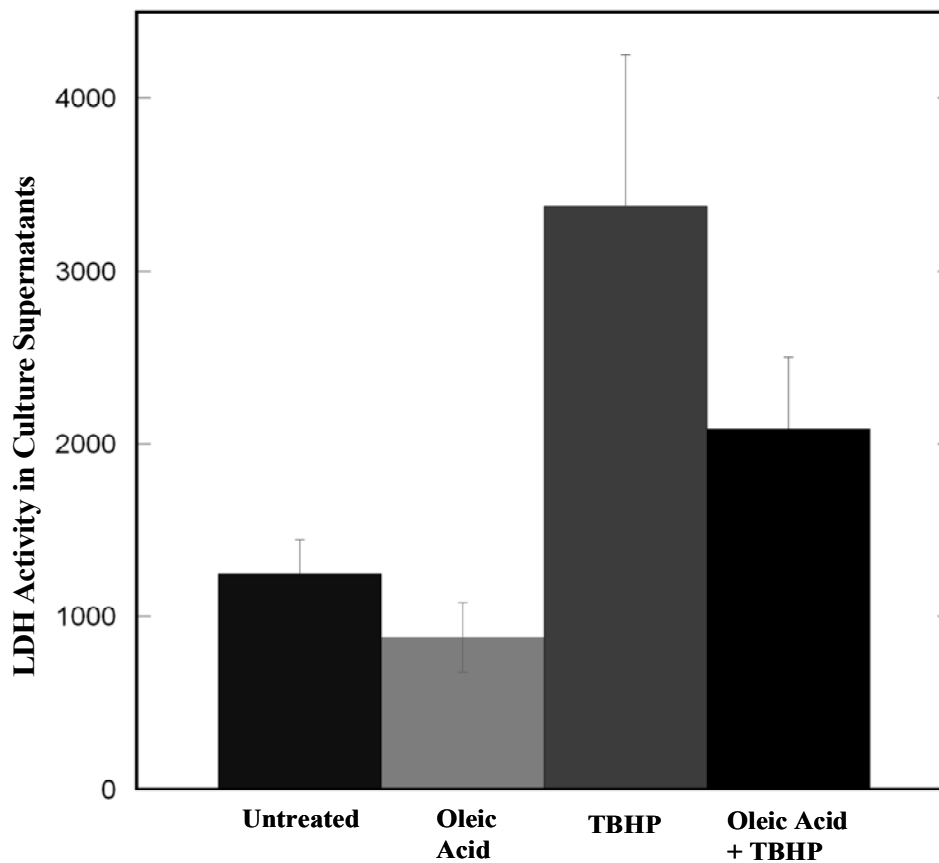
Figure 6. LDH activity in HepG2 culture supernatants exposed to 0.15 mM oleic acid for 48 hr and then to 500 μM TBHP for 8 hr.

4.4 Cytokine Inflammation in Fat-loaded HepG2 Cells

It has been proposed that during AS, hepatocytes become sensitized to the effects of cytokines (9-11), which leads to steatohepatitis (i.e., a 2-hit model). Therefore, we investigated the extent of inflammation in fat-loaded hepatocytes reporter cells by monitoring the activation of the transcription factor NF-κB by the cytokine TNF-α. This is a relevant model as TNF- α is well established to be present during steatohepatitis and NF-κB is a known pro-inflammatory transcription factor. Experiments were carried out

using rat hepatoma (H35) GFP-reporter cells for NF-κB (60). Reporter cells were loaded

with 0.15 or 0.90 mM oleic acid for 48 h and exposed to 10 ng/mL of TNFα. Activation

of NF-κB leads to expression of GFP from the minimal CMV promoter and

fluorescence, which was continuously monitored using fluorescence microscopy. The

data in Figure 7 show that the 0.15 and 0.90 mM oleic acid treated cells displayed

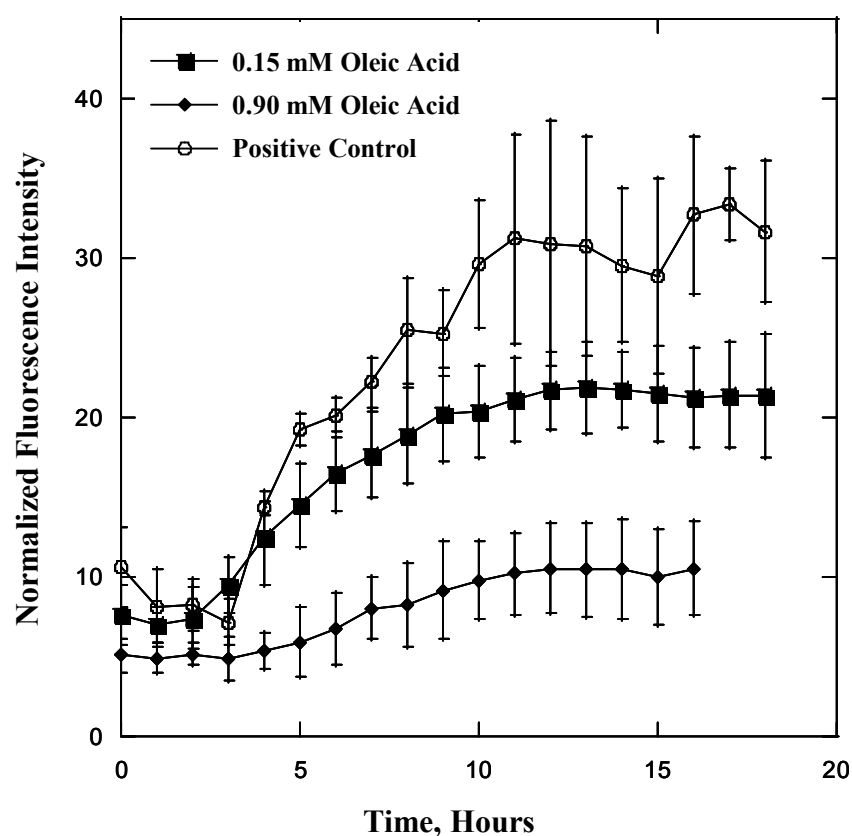approximately 33% and 67% less florescence than the normal HepG2 cells,

Figure 7. H35 reporter cells expressing NF-κB linked GFP. H35 cells were fat
loaded with oleic acid for 48 hr and the exposed to 25 nM TNFα for 24 hours.
Fluorescence intensity was measured every hour.

suggesting that TNF-α−mediated NF-κB activation is attenuated in the fat loaded cells. This result is consistent with the LDH cytotoxicity assay results showing that fat-loaded cells are less susceptible to oxidative stress.

4.5 Isolation and Identification of Carbonylated Proteins

Carbonylated proteins from TBHP-treated fat-loaded or control HepG2 cells were tagged with biotin hydrazide and affinity purified using monomeric avidin-linked beads as described in Materials & Methods. The lysis buffer for this procedure contained components that were all dialyzable and did not contain amines (e.g. Tris) that could compete with the biotin hydrazide for Schiff base formation. The protocol used was adapted from Mirzai *et al* (20), with the main difference being that procedure was conducted in semi-batch mode using disposable centrifuge spin columns. Equal amounts of protein from TBHP-treated control or fat-loaded HepG2 cells were loaded onto each column, bound to the monomeric avidin in the column, and eluted as described in M&M. Quantification of the eluted (carbonylation) protein showed that cells treated with 0.15 mM oleic acid prior to TBHP exposure had 17% less carbonylated protein than normal cells exposed to TBHP, and indicated that carbonylated protein levels were decreased in the oleic acid-loaded samples upon TBHP exposure as compared to normal cells. However, this measurement of carbonylated protein content does not provide any information on the extent of carbonylation of specific proteins. Therefore, mass spectrometry was used to identify carbonylated proteins in normal and fat-loaded HepG2 cells exposed to TBHP.

Parallel samples from TBHP-treated fat-loaded or control cells were purified and separated on 8-16% SDS PAGE using standard protocols and visualized using Sypro Red staining. Qualitative inspection of the gel image (Figure 8), as well as quantification of the overall protein in the gel (not shown) by densitometry was consistent with the Bradford assay results (i.e. less protein was present in TBHP-exposed fat-loaded cells compared to normal controls). Each lane in the gel was cut into 36 evenly spaced slices of 1-2 mm. Proteins in each gel slice were digested in-gel with trypsin, and subjected to LC-MS/MS analysis. The mass spectrometry data show that 249 carbonylated proteins were identified from the non fat loaded TBHP treated cells, while only 119 proteins were identified from TBHP-treated fat loaded cells. Only 24 proteins were common between the two samples (Figure 9). Since carbonylated proteins are typically cleared from cells through the proteasomal/ubiquitin system or aggregate in the cell, leading to cellular dysfunction, a decrease in carbonylation is an indicator of increased resistance to oxidative stress. The overall trend of finding fewer carbonylated proteins in the fat loaded sample is consistent with the data from the Bradford assay and the gel density measurement showing less carbonyl content with fat loading.
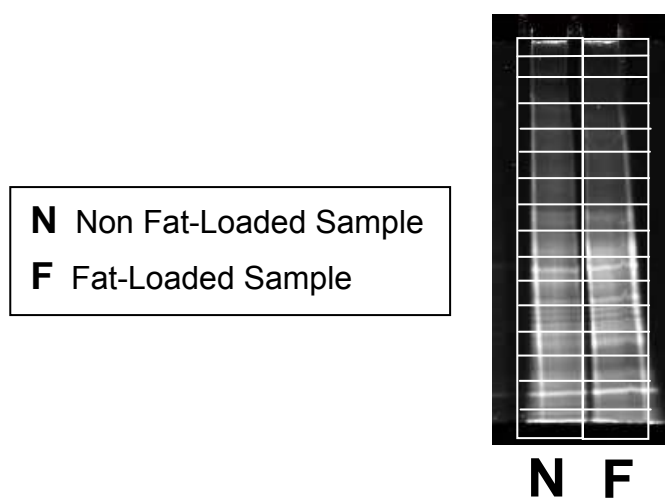
Figure 8. Carbonylated proteins resolved on an 8-16% acrylamide gel. Gel lane containing non fat-loaded (N) sample showed average density of 17% less than the fat loaded sample (F).
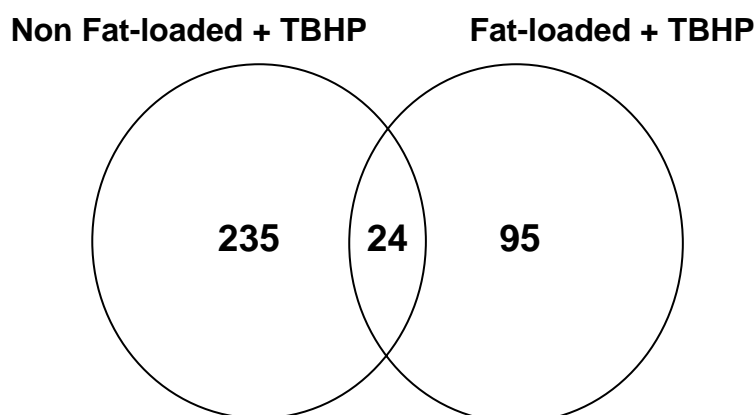
Figure 9. Distribution of carbonylated proteins in normal and fat-loaded HepG2 cells.

Selected proteins belonging to different functional categories (e.g., metabolism) that were carbonylated in either of the experimental groups are listed in Table 2. Cytoskeletal proteins were identified in both experimental groups; this is expected as these are highly abundant and are likely more susceptible to attack by ROS (70).

Table 2. Carbonylated proteins detected in normal and fat-loaded HepG2 cells.

| Protein Category and Name	Accession No.	Experimental Group in which Protein Detected	
		Non Fat Loaded + TBHP	Fat Loaded + TBHP
Metabolism Proteins			
Fructose-bisphosphate aldolase A	P05062	-	+
Potassium-transporting ATPase alpha chain 2	P54707	+	-
Malate dehydrogenase (mp)	P40926	+	-
Glyceraldehyde-3-phosphate dehydrogenase	P04406	+	-
Fat Transport and Synthesis Proteins			
Long chain acyl coA ligase	P33121	+	-
ATP-binding cassette sub-family A member 1	O95477	+	-
2-acylglycerol O-acyltransferase 1	Q96PD6	+	-
Long-chain fatty acid transport protein 6	Q9Y2P4	-	+
Cytoskeletal Proteins			
Collagen	Q01955	+	-
Catenin	P26232	+	-
Myosin V	P35580	+	+
Actin, cytoplasmic 2	P63261	+	+
Antioxidant Proteins			
Thioredoxin reductase 1	Q16881	-	+
Chaperone Proteins			
Peptidyl-prolyl cis-trans isomerase	P68106	+	-
HSP10	P61604	+	-
HSP75	Q12931	+	-
DnaJ homolog	P59910	+	-
Protein disulfide-isomerase precursor	P07237	+	-
Heat shock 70 kDa protein 4	P34932	-	+
Heat-shock protein 105 kDa	Q92598	-	+
Ubitiquin & Drug Resistance Protein			
Ubiquitin carboxyl-terminal hydrolase 34	Q70CQ2	+	-
E3 ubiquitin-protein ligase UBR1	Q8IWV7	+	-
Probable E3 ubiquitin-protein ligase MYCBP2	O75592	+	-
Multidrug resistance-associated protein 7	Q5T3U5	+	-

It is interesting to note that long-chain fatty acid binding protein 6 was carbonylated only in the oleic acid treated sample. It is unclear whether this protein exhibits greater than average susceptibility to carbonylation or if simply greater quantities were induced by the fat-loading.

Chaperone proteins are common targets of ROS attack and researchers have identified damaged or malfunctioning chaperone proteins as part cellular pathologies (71). Peptidyl-prolyl cis-trans isomerase is an abundant and ubiquitous folding protein that catalyzes the cis-trans isomerization of certain proline residues (72). The fact that these proteins are carbonylated in normal HepG2 cells but not in oleic-loaded cells further supports the hypothesis that oleic acid-loading protects HepG2 cells against TBHP-induced oxidative stress.

5. DISCUSSION, SUMMARY, AND CONCLUSIONS

Alcoholic liver disease is a significant public health problem and costs associated with alcoholism are approximately $185 billion annually (23). The major pathologies of ALD are alcoholic steaotosis, alcoholic steatohepatitis, and upon continued ethanol consumption, fibrosis and cirrhosis. Steatosis represents an attractive target for understanding the molecular basis of ALD not only because there is a lack of understanding of molecular mechanisms underlying this disease, but also of its subsequent progression to ASH and end-stage liver disease. From a clinical stand point, targeting AS for diagnosis and treatment is desirable, because once ALD progresses to ASH, only 10% of livers revert back to normal (40).

Our 2DE-MS analysis identified 18 proteins as differentially expressed between the ethanol and control groups (Table 1). Interestingly, these 18 spots were detected in both the 3 weeks and 6 weeks ethanol fed groups. The observation that proteins characterizing steatosis at 3 weeks are also differentially expressed at 6 weeks suggests changes in protein expression occur rapidly during the development of AS. The modest changes in expression between the 3 weeks group and the 6 weeks ethanol fed group also suggests that effect of ethanol on protein expression levels off after 3 weeks; however, prior reports (1) have shown that extensive pathological changes are observed only after 6 weeks of alcohol exposure. Together, our data are consistent with the notion that alcohol consumption rapidly induces steatosis (1, 2).

Alcohol consumption up-regulated the expression of proteins involved in fat and amino acid metabolism, and likely reflects increased cellular demand for energy in AS.

One possible source for increased energy requirements is the response to alcohol-induced oxidative stress. Increased ATP requirement would be expected during oxidative stress, as several studies (73, 74) have linked ATP depletion with oxidative stress and related cellular damage. Acyl-CoA dehydrogenase and delta3,5-delta2, 4-dienoyl-CoA isomerase are both involved in mitochondrial beta oxidation of fatty acids (63, 64).   The former catalyzes the first step of beta oxidation, and the latter is necessary for the beta oxidation of unsaturated fatty acids, namely docosahexaenoic acid (64). It is interesting that these enzymes are upregulated, as the depletion of NAD+ from ethanol and acetaldehyde metabolism is thought to interfere with fatty acid metabolism (75). 3-hydroxyisobutyrate dehydrogenase is necessary for branched chain amino acid catabolism (65) and its increase also suggests an increased energy requirement. The increase in ADP/ATP translocase 2 (involved in the movement of ATP and ADP across the mitochondrial membrane) also supports the AS induced increase in cellular energy production. It would interesting to verify increased fatty acid beta oxidation and ATP generation during AS.

The expression levels of ALDH2 and PRDX6 are reduced in the ethanol treated group compared to the control group. While one might expect that a state of oxidative stress induces an increase in the expression of anti-oxidant systems, several studies have actually reported that key enzymes involved in counteracting the effects of oxidative stress are actually reduced during oxidative stress, and thus their reduced expression actually indicates a state of oxidative stress. A recent study (76) also showed that mitochondrial proteins (e.g. ALDH2) of alcohol-fed rats were oxidatively modified and

nitrosylated, and that the enzymatic function of these proteins was reduced. It has been suggested that the cysteine residues and metal centers found at the active sites of many anti-oxidant and metabolism proteins makes them more vulnerable to ROS attack (76, 77). The expression levels of such oxidatively-modified proteins are often decreased, as has been demonstrated for glutathione S-transferase A4 (GSTA4) in obese mice (78). Therefore, it is possible most of the decrease in PRDX6 and ALDH2 is due to increased carbonylation. Together, these changes in protein expression clearly indicate an increased state of oxidative stress in AS.

Our data showing an increase in enzymes involved fatty acid oxidation (acyl-CoA dehydrogenase and delta3,5-delta2, 4-dienoyl-CoA isomerase) is contrary to the generally accepted view that AS results in decreased fatty acid oxidation. This motivated the development of an *in vitro* experimental model that would allow the investigation of the effects of fat accumulation and oxidative stress separately.   A fat loading hepatocyte cell culture model was developed using the HepG2 human hepatoblastoma cell line with oleic acid as the model fatty acid. Our observations on oleic acid-loaded HepG2 cells being less susceptible to TBHP-induced oxidative stress and TNF-α induced inflammation is surprising as the accumulation of fat is generally associated with increased susceptibility to oxidative stress (9-11). However these results are in agreement with a recent study (67) that also reported that fat-loaded HepG2 spheroids were less susceptible to oxidative challenge and inflammation.   However, it is also possible that the effect of fat loading depends on the type of fatty acid used. Prior work by Nanji et al. (7) has shown that the severity of ALD pathology in alcohol fed

rats correlates to the amount of linoleic acid in the diet. This is also supported by Gomez-Lechon et al. (68) who demonstrated that composition and concentration of fatty acid loading is important in determining fat loading toxicity. The authors show that fat loading hepatocytes with 0.5 mM oleic acid for 24 hours did not significantly reduce cell viability, but fat loading with 1.0 mM palmitic acid reduced cell viability by 40%. Thus, development of an accurate model representing fat accumulation in AS likely depends on fatty acid composition and concentration. Investigating the effect of different fatty acids (palmitic, linoleic) as well as combinations of fatty acids is a logical next line of investigation.

Based on our data showing that oxidative stress is a key determinant of protein expression changes in AS, we hypothesized that carbonyl modification of proteins will also be significant during AS and can explain the down-regulation of anti-oxidant enzymes such as PRDX6 and ALDH2. Carbonylation is a widely prevalent irreversible oxidative modification of proteins (70), and it is known that carbonylated proteins are susceptible to ubiquitination and subsequent degradation by proteosomal/lyosomal pathways (79, 80). Our findings on less carbonylated proteins being present in oleic acid-loaded HepG2 cells is also in good agreement with cytotoxicity and inflammation assays. Our results (Figure 8) show that a majority of carbonylated proteins are found towards the bottom of the gel. (i.e., below 45 kilodaltons). This indicates that the majority of detected carbonylated proteins were fragmented, and is likely the result of increased degradation (as would be expected with carbonylated proteins).

It is not surprising that a broad spectrum of proteins (cytoskeleton, metabolism, fatty acid synthesis and transport) were all carbonylated, as the oxidant exposure likely produces an even distribution of TBHP and subjects a broad range of proteins to oxidative damage. Many chaperone proteins were carbonylated (Table 2), and our data show reduced levels of chaperone proteins Hsc70 and Erp29. Chaperone proteins are common targets of ROS attack and researchers have identified damaged or malfunctioning chaperone proteins as part cellular pathologies (71). Peptidyl-prolyl cis-trans isomerase is an abundant and ubiquitous folding protein that catalyzes the cis-trans isomerization of certain proline residues (72). Chaperone proteins are involved in protein folding and have been reported as vulnerable to oxidative stress (70), and this supports the finding that mice fed ethanol intragastrically developed protein misfolding response and endoplasmic reticulum stress (81). The fact that several ubiquitin related proteins were carbonylated suggests a reduced ability to clear damaged proteins and may contribute to the formation of protein aggregates associated with oxidized proteins (20, 21, 70, 81). Similarly, it is also possible that excessive degradation or dysfunction of fatty acid transport and synthesis proteins contribute to the possible toxic effects fat accumulation, and explains the association of increased fat accumulation with increased oxidative stress in alcoholic steatosis.

Development of an *in vitro* fat loading hepatocyte model actually demonstrated that fat loading with low concentration oleic acid actually produces enhanced protection against oxidative stress and TNF-α induced inflammatory response. It thus appears that *in vitro* fat-loading in order to accurately mimic fat accumulation during alcoholic

steatosis is a complex and multi-variate phenomenon and requires careful consideration. Further directions in this regard include evaluating the effect of different fatty acids, both individually and in combination.

The identification of carbonylated proteins yielded interesting results and suggested chaperone, ubutiquin, and fatty acid transport and synthesis proteins are vulnerable to carbonylation during a state of oxidative stress. Future work in this area will focus on determining if these carbonylated proteins are decreased in expression using quantitative iTRAQ mass spectrometry (82). This, coupled with multi-dimensional protein identification approaches such as liquid chromatography, will generate a more quantitative picture of protein modifications during oxidative stress.

REFERENCES

1. Ramaiah, S., Rivera, C., and Arteel, G. (2004) Early-phase alcoholic liver disease: an update on animal models, pathology, and pathogenesis. *Int. J. Toxicol.* **23**, 217-231.

2. Diehl, A. M. (2002) Liver disease in alcohol abusers: clinical perspective. *Alcohol* **27**, 7-11.

3. Galambos, J. T. (1972) Natural history of alcoholic hepatitis. 3. Histological changes. *Gastroenterology* **63**, 1026-1035.

4. Pares, A., Caballeria, J., Bruguera, M., Torres, M., and Rodes, J. (1986) Histological course of alcoholic hepatitis. Influence of abstinence, sex and extent of hepatic damage. *J. Hepatol.* **2**, 33-42.

5. MacSween, R. N., and Burt, A. D. (1986) Histologic spectrum of alcoholic liver disease. *Semin. Liver Dis.* **6**, 221-232.

6. Day, C. P., and James, O. F. (1998) Hepatic steatosis: innocent bystander or guilty party? *Hepatology* **27**, 1463-1466.

7. Nanji, A. A., Mendenhall, C. L., and French, S. W. (1989) Beef fat prevents alcoholic liver disease in the rat. *Alcohol Clin. Exp. Res.* **13**, 15-19.

8. Sorensen, T. I., Orholm, M., Bentsen, K. D., Hoybye, G., Eghoje, K., and Christoffersen, P. (1984) Prospective evaluation of alcohol abuse and alcoholic liver injury in men as predictors of development of cirrhosis. *Lancet* **2**, 241-244.

9.   Bykov, I., Jarvelainen, H., and Lindros, K. (2003) L-carnitine alleviates alcohol-induced liver damage in rats: role of tumour necrosis factor-alpha. *Alcohol Alcohol* **38**, 400-406.

10.   Colell, A., Garcia-Ruiz, C., Miranda, M., Ardite, E., Mari, M., Morales, A., Corrales, F., Kaplowitz, N., and Fernandez-Checa, J. C. (1998) Selective glutathione depletion of mitochondria by ethanol sensitizes hepatocytes to tumor necrosis factor. *Gastroenterology* **115**, 1541-1551.

11.   Yang, S. Q., Lin, H. Z., Lane, M. D., Clemens, M., and Diehl, A. M. (1997) Obesity increases sensitivity to endotoxin liver injury: implications for the pathogenesis of steatohepatitis. *Proc. Natl. Acad. Sci. U S A* **94**, 2557-2562.

12.   Teli, M. R., Day, C. P., Burt, A. D., Bennett, M. K., and James, O. F. (1995) Determinants of progression to cirrhosis or fibrosis in pure alcoholic fatty liver. *Lancet* **346**, 987-990.

13.   Wurst, F. M., Kempter, C., Metzger, J., Seidl, S., and Alt, A. (2000) Ethyl glucuronide: a marker of recent alcohol consumption with clinical and forensic implications. *Alcohol* **20**, 111-116.

14.   Galasko, D. (2005) Biomarkers for Alzheimer's disease--clinical needs and application. *J. Alzheimers Dis.* **8**, 339-346.

15.   Kasinathan, C., Vrana, K., Beretta, L., Thomas, P., Gooch, R., Worst, T., Walker, S., Xu, A., Pierre, P., Green, H., Grant, K., and Manowitz, P. (2004) The future of proteomics in the study of alcoholism. *Alcohol Clin. Exp. Res.* **28**, 228-232.

16. Anni, H., and Israel, Y. (1999) Characterization of adducts of ethanol metabolites with cytochrome c. *Alcohol Clin. Exp. Res.* **23**, 26-37.

17. NIAAA (2003) The genetics of alcoholism. *Alcohol Alerts*, 60 Ed., National Institute on Alcohol Abuse and Alcoholism.

18. Witzmann, F. A., and Strother, W. N. (2004) Proteomics and alcoholism. *Int. Rev. Neurobiol.* **61**, 189-214.

19. Soreghan, B. A., Yang, F., Thomas, S. N., Hsu, J., and Yang, A. J. (2003) High-throughput proteomic-based identification of oxidatively induced protein carbonylation in mouse brain. *Pharm. Res.* **20**, 1713-1720.

20. Mirzaei, H., and Regnier, F. (2005) Affinity chromatographic selection of carbonylated proteins followed by identification of oxidation sites using tandem mass spectrometry. *Anal. Chem.* **77**, 2386-2392.

21. Mirzaei, H., and Regnier, F. (2007) Identification of yeast oxidized proteins: chromatographic top-down approach for identification of carbonylated, fragmented and cross-linked proteins in yeast. *J. Chromatogr. A.* **1141**, 22-31.

22. He, Y., Yang, F., Wang, F., Song, S. X., Li, D. A., Guo, Y. J., and Sun, S. H. (2007) The upregulation of expressed proteins in HepG2 cells transfected by the recombinant plasmid-containing HBx gene. *Scand J Immunol* **65**, 249-256.

23. NIAAA (2001) Economic perspectives in alcoholism research. *Alcohol Alerts*, No. 51 Ed., National Institute on Alcohol Abuse and Alcoholism

24. Arteel, G., Marsano, L., Mendez, C., Bentley, F., and McClain, C. J. (2003) Advances in alcoholic liver disease. *Best Pract. Res. Clin. Gastroenterol* **17**, 625-647.

25. Arteel, G. E. (2003) Oxidants and antioxidants in alcohol-induced liver disease. *Gastroenterology* **124**, 778-790.

26. Brunt, E. M., and Tiniakos, D. G. (2002) Pathology of steatohepatitis. *Best Pract. Res. Clin. Gastroenterol* **16**, 691-707.

27. Ishak, K. G., Zimmerman, H. J., and Ray, M. B. (1991) Alcoholic liver disease: pathologic, pathogenetic and clinical aspects. *Alcohol Clin. Exp. Res.* **15**, 45-66.

28. Lieber, C. S. (1993) Biochemical factors in alcoholic liver disease. *Semin. Liver Dis.* **13**, 136-153.

29. Lieber, C. S. (1994) Alcohol and the liver: 1994 update. *Gastroenterology* **106**, 1085-1105.

30. Maher, J. J. (2002) Alcoholic steatosis and steatohepatitis. *Semin. Gastrointest. Dis.* **13**, 31-39.

31. Zhao, L. F., Jia, J. M., and Han, D. W. (2004) The role of enterogenous endotoxemia in the pathogenesis of non-alcoholic steatohepatitis. *Zhonghua Gan Zang Bing Za Zhi* **12**, 632-638.

32. Donohue, T. M., Jr. (2007) Alcohol-induced steatosis in liver cells. *World J. Gastroenterol.* **13**, 4974-4978.

33. Desmet, V. J. (1985) Alcoholic liver disease. Histological features and evolution. *Acta Med. Scand. Suppl.* **703**, 111-126.

34.   Burt, A. D., and MacSween, R. N. (1986) Hepatic vein lesions in alcoholic liver

disease: retrospective biopsy and necropsy study. *J. Clin. Pathol.* **39**, 63-67.

35.   Fischer, M., You, M., Matsumoto, M., and Crabb, D. W. (2003) Peroxisome

proliferator-activated receptor alpha (PPARalpha) agonist treatment reverses

PPARalpha dysfunction and abnormalities in hepatic lipid metabolism in

ethanol-fed mice. *J. Biol. Chem.* **278**, 27997-28004.

36.   Galli, A., Pinaire, J., Fischer, M., Dorris, R., and Crabb, D. W. (2001) The

transcriptional and DNA binding activity of peroxisome proliferator-activated

receptor alpha is inhibited by ethanol metabolism. A novel mechanism for the

development of ethanol-induced fatty liver. *J. Biol. Chem.* **276**, 68-75.

37.   Apte, U. M., McRee, R., and Ramaiah, S. K. (2004) Hepatocyte proliferation is

the possible mechanism for the transient decrease in liver injury during steatosis

stage of alcoholic liver disease. *Toxicol. Pathol.* **32**, 567-576.

38.   Bautista, A. P. (2002) Neutrophilic infiltration in alcoholic hepatitis. *Alcohol* **27**,

17-21.

39.   Jaeschke, H. (2002) Neutrophil-mediated tissue injury in alcoholic hepatitis.

Alcohol **27**, 23-27.

40.   French, S. W. (2002) Alcoholic hepatitis: inflammatory cell-mediated

hepatocellular injury. *Alcohol* **27**, 43-46.

41.   McCord, J. M., and Fridovich, I. (1969) Superoxide dismutase. An enzymic

function for erythrocuprein (hemocuprein). *J. Biol. Chem.* **244**, 6049-6055.

42. Kessova, I. G., Ho, Y. S., Thung, S., and Cederbaum, A. I. (2003) Alcohol-induced liver injury in mice lacking Cu, Zn-superoxide dismutase. *Hepatology* **38**, 1136-1145.

43. Fridovich, I. (1995) Superoxide radical and superoxide dismutases. *Annu. Rev. Biochem.* **64**, 97-112.

44. Klebanoff, S. J. (1968) Myeloperoxidase-halide-hydrogen peroxide antibacterial system. *J Bacteriol.* **95**, 2131-2138.

45. Beckman, J. S., Beckman, T. W., Chen, J., Marshall, P. A., and Freeman, B. A. (1990) Apparent hydroxyl radical production by peroxynitrite: implications for endothelial injury from nitric oxide and superoxide. *Proc Natl Acad Sci USA* **87**, 1620-1624.

46. Lieber, C. S. (2000) Hepatic, metabolic, and nutritional disorders of alcoholism: from pathogenesis to therapy. *Crit. Rev. Clin. Lab. Sci.* **37**, 551-584.

47. Cederbaum, A. I., Wu, D., Mari, M., and Bai, J. (2001) CYP2E1-dependent toxicity and oxidative stress in HepG2 cells. *Free Radic. Biol. Med.* **31**, 1539-1543.

48. Esterbauer, H., Schaur, R. J., and Zollner, H. (1991) Chemistry and biochemistry of 4-hydroxynonenal, malonaldehyde and related aldehydes. *Free Radic. Biol. Med.* **11**, 81-128.

49. Dalle-Donne, I., Scaloni, A., Giustarini, D., Cavarra, E., Tell, G., Lungarella, G., Colombo, R., Rossi, R., and Milzani, A. (2005) Proteins as biomarkers of

oxidative/nitrosative stress in diseases: the contribution of redox proteomics. *Mass Spectrom. Rev.* **24**, 55-99.

50.   Levine, R. L., Moskovitz, J., and Stadtman, E. R. (2000) Oxidation of methionine in proteins: roles in antioxidant defense and cellular regulation. *IUBMB Life* **50**, 301-307.

51.   Dalle-Donne, I., Giustarini, D., Colombo, R., Milzani, A., and Rossi, R. (2005) S-glutathionylation in human platelets by a thiol-disulfide exchange-independent mechanism. *Free Radic. Biol. Med.* **38**, 1501-1510.

52.   Yan, L. J., Levine, R. L., and Sohal, R. S. (1997) Oxidative damage during aging targets mitochondrial aconitase. *Proc Natl Acad Sci USA* **94**, 11168-11172.

53.   Yan, L. J., and Sohal, R. S. (1998) Mitochondrial adenine nucleotide translocase is modified oxidatively during aging. *Proc Natl Acad Sci USA* **95**, 12896-12901.

54.   Das, N., Levine, R. L., Orr, W. C., and Sohal, R. S. (2001) Selectivity of protein oxidative damage during aging in Drosophila melanogaster. *Biochem J.* **360**, 209-216.

55.   England, K., and Cotter, T. (2004) Identification of carbonylated proteins by MALDI-TOF mass spectroscopy reveals susceptibility of ER. *Biochem. Biophys. Res. Commun.* **320**, 123-130.

56.   Rabek, J. P., Boylston, W. H., 3rd, and Papaconstantinou, J. (2003) Carbonylation of ER chaperone proteins in aged mouse liver. *Biochem. Biophys. Res. Commun.* **305**, 566-572.

57. Chaudhuri, A. R., de Waal, E. M., Pierce, A., Van Remmen, H., Ward, W. F., and Richardson, A. (2006) Detection of protein carbonyls in aging liver tissue: A fluorescence-based proteomic approach. *Mech. Ageing Dev.* **127**, 849-861.

58. Deaciuc, I. V., D'Souza, N. B., Burikhanov, R., Lee, E. Y., Tarba, C. N., McClain, C. J., and de Villiers, W. J. (2002) Epidermal growth factor protects the liver against alcohol-induced injury and sensitization to bacterial lipopolysaccharide. *Alcohol Clin. Exp. Res.* **26**, 864-874.

59. Enomoto, N., Yamashina, S., Kono, H., Schemmer, P., Rivera, C. A., Enomoto, A., Nishiura, T., Nishimura, T., Brenner, D. A., and Thurman, R. G. (1999) Development of a new, simple rat model of early alcohol-induced liver injury based on sensitization of Kupffer cells. *Hepatology* **29**, 1680-1689.

60. King, K. R., Wang, S., Irimia, D., Jayaraman, A., Toner, M., and Yarmush, M. L. (2007) A high-throughput microfluidic real-time gene expression living cell array. *Lab Chip* **7**, 77-85.

61. Colditz, F., Nyamsuren, O., Niehaus, K., Eubel, H., Braun, H. P., and Krajinski, F. (2004) Proteomic approach: identification of Medicago truncatula proteins induced in roots after infection with the pathogenic oomycete Aphanomyces euteiches. *Plant Mol Biol* **55**, 109-120.

62. Laemmli, U. K., Beguin, F., and Gujer-Kellenberger, G. (1970) A factor preventing the major head protein of bacteriophage T4 from random aggregation. *J. Mol. Biol.* **47**, 69-85.

63. Pace, C. P., and Stankovich, M. T. (1994) Oxidation-reduction properties of short-chain acyl-CoA dehydrogenase: effects of substrate analogs. *Arch. Biochem. Biophys.* **313**, 261-266.

64. Sprecher, H. (1996) New advances in fatty-acid biosynthesis. *Nutrition* **12**, S5-7.

65. Hu, H., Jaskiewicz, J. A., and Harris, R. A. (1992) Ethanol and oleate inhibition of alpha-ketoisovalerate and 3-hydroxyisobutyrate metabolism by isolated hepatocytes. *Arch. Biochem. Biophys.* **299**, 57-62.

66. Simeone, M., and Phelan, S. A. (2005) Transcripts associated with Prdx6 (peroxiredoxin 6) and related genes in mouse. *Mamm. Genome* **16**, 103-111.

67. Damelin, L. H., Coward, S., Kirwan, M., Collins, P., Selden, C., and Hodgson, H. J. (2007) Fat-loaded HepG2 spheroids exhibit enhanced protection from Pro-oxidant and cytokine induced damage. *J. Cell. Biochem.* **101**, 723-734.

68. Gomez-Lechon, M. J., Donato, M. T., Martinez-Romero, A., Jimenez, N., Castell, J. V., and O'Connor, J. E. (2007) A human hepatocellular *in vitro* model to investigate steatosis. *Chem. Biol. Interact.* **165**, 106-116.

69. Alia, M., Ramos, S., Mateos, R., Bravo, L., and Goya, L. (2005) Response of the antioxidant defense system to tert-butyl hydroperoxide and hydrogen peroxide in a human hepatoma cell line (HepG2). *J. Biochem. Mol. Toxicol.* **19**, 119-128.

70. Dalle-Donne, I., Aldini, G., Carini, M., Colombo, R., Rossi, R., and Milzani, A. (2006) Protein carbonylation, cellular dysfunction, and disease progression. *J. Cell Mol. Med.* **10**, 389-406.

71. Crabb, D. W. (2004) Alcohol Deranges Hepatic Lipid Metabolism via Altered Transcriptional Regulation. *Trans. Am. Clin. Climatol. Assoc.* **115**, 273-287.

72. Ou, W. B., Luo, W., Park, Y. D., and Zhou, H. M. (2001) Chaperone-like activity of peptidyl-prolyl cis-trans isomerase during creatine kinase refolding. *Protein Sci.* **10**, 2346-2353.

73. Almeida, A., and Bolanos, J. P. (2001) A transient inhibition of mitochondrial ATP synthesis by nitric oxide synthase activation triggered apoptosis in primary cortical neurons. *J. Neurochem.* **77**, 676-690.

74. O'Brien, P. J., Chan, K., and Silber, P. M. (2004) Human and animal hepatocytes *in vitro* with extrapolation *in vivo*. *Chem. Biol. Interact.* **150**, 97-114.

75. Donohue, T. M., Curry-McCoy, T. V., Nanji, A. A., Kharbanda, K. K., Osna, N. A., Radio, S. J., Todero, S. L., White, R. L., and Casey, C. A. (2007) Lysosomal leakage and lack of adaptation of hepatoprotective enzyme contribute to enhanced susceptibility to ethanol-induced liver injury in female rats. *Alcohol Clin. Exp. Res.* **31**, 1944-1952.

76. Moon, K. H., Hood, B. L., Kim, B. J., Hardwick, J. P., Conrads, T. P., Veenstra, T. D., and Song, B. J. (2006) Inactivation of oxidized and S-nitrosylated mitochondrial proteins in alcoholic fatty liver of rats. *Hepatology* **44**, 1218-1230.

77. Stadtman, E. R. (1992) Protein oxidation and aging. *Science* **257**, 1220-1224.

78. Grimsrud, P. A., Picklo, M. J., Sr., Griffin, T. J., and Bernlohr, D. A. (2007) Carbonylation of adipose proteins in obesity and insulin resistance: identification

of adipocyte fatty acid-binding protein as a cellular target of 4-hydroxynonenal. *Mol. Cell. Proteomics* **6**, 624-637.

79.   Shang, F., Nowell, T. R., Jr., and Taylor, A. (2001) Removal of oxidatively damaged proteins from lens cells by the ubiquitin-proteasome pathway. *Exp. Eye Res.* **73**, 229-238.

80.   Marques, C., Pereira, P., Taylor, A., Liang, J. N., Reddy, V. N., Szweda, L. I., and Shang, F. (2004) Ubiquitin-dependent lysosomal degradation of the HNE-modified proteins in lens epithelial cells. *Faseb J.* **18**, 1424-1426.

81.   Kaplowitz, N., and Ji, C. (2006) Unfolding new mechanisms of alcoholic liver disease in the endoplasmic reticulum. *J. Gastroenterol. Hepatol.* **21 Suppl 3**, S7-9.

82.   Meany, D. L., Xie, H., Thompson, L. V., Arriaga, E. A., and Griffin, T. J. (2007) Identification of carbonylated proteins from enriched rat skeletal muscle mitochondria using affinity chromatography-stable isotope labeling and tandem mass spectrometry. *Proteomics* **7**, 1150-1163.

VITA

Billy Walker Newton received his Bachelor of Science degree in chemical engineering from Texas A&M University in 2000. He entered the chemical engineering graduate program at Texas A&M University in January 2005, and graduated with his M.S. in May 2008. His research interests include proteomics and studying the biological effects of oxidative stress.

Name: Billy Walker Newton

Address: Chemical Engineering, 3122 TAMU, College Station, TX, 77843-3122

Email Address: bwn2869@chemail.tamu.edu

Education: B.S., Chemical Engineering, Texas A&M University, 2000
               M.S., Chemical Engineering, Texas A&M University, 2008